Electronic Supplementary Material (ESI) for Chemical Science.
This journal is © The Royal Society of Chemistry 2017

Supplementary Information for

Apoptosis-Independent Organoruthenium Anticancer Complexes that Overcome Multidrug Resistance: Self-Assembly and Phenotypic Screening Strategies

Mun Juinn Chow[*,1], *Mohammad Alfiean*[2], *Giorgia Pastorin*[3,4], *Christian Gaiddon*[5,6] *and Wee Han Ang*[*,1,4]

[1]Department of Chemistry, National University of Singapore, 3 Science Drive 3, 117543 Singapore

[2]School of Chemistry and Life Sciences, Nanyang Polytechnic, Singapore

[3]Department of Pharmacy, National University of Singapore, 3 Science Drive 3, 117543 Singapore

[4]NUS Graduate School for Integrative Sciences and Engineering, Singapore

[5]Université de Strasbourg, Strasbourg, France

[6]U1113 INSERM, 3 Avenue Molière, Strasbourg 67200, France

*corresponding authors

EXPERIMENTAL

Materials. All experimental procedures were carried out without additional precautions to exclude air or moisture unless otherwise specified. All chemicals and solvents were used as received. $RuCl_3.xH_2O$ was purchased from both Precious Metals Online. $[(\eta^6$-hexamethylbenzene)$RuCl_2]_2$ and $[(\eta^6$-1,3,5-triisopropylbenzene)$RuCl_2]_2$ were synthesized according to previously reported protocols.[1] Thiazolyl blue tetrazolium bromide (MTT), IGEPAL CA-630, DL-Dithiothreitol, Tetramethylethylenediamine (TEMED), Sodium Deoxycholate, Non-fat Dried Milk Bovine, Bovine Serum Albumin, TWEEN® 20 and Ponceau S were purchased from Sigma-Aldrich. Tris was purchased from Vivantis Technologies. Gibco® MEM Non-Essential Amino Acids solution (NEAA) and 10% SDS solution were purchased from Life Technologies. Glycine, Hyclone™ Trypsin Protease 2.5% (10X) solution, RPMI 1640, DMEM medium, Fetal bovine serum (FBS) and Pierce™ Protease and Phosphatase Inhibitor Mini Tablets were purchased from Thermo Fisher Scientific. Hyclone™ Dulbecco's Phosphate-Buffered Saline (10x) and Penicillin-Streptomycin (10 000 U/mL) were purchased from Ge Healthcare Life Sciences. Bio-rad Protein Assay Dye Reagent Concentrate, 30% Acrylamide/Bis solution, 4x Laemmli Sample Buffer, Nitrocellulose Membrane, 0.2 µm and 0.45 µm were purchased from Bio-rad Laboratories. Luminata™ Classico, Crescendo and Forte Western HRP Substrate were purchased from Merck Millipore Corporation. Pan Caspase Inhibitor z-VAD-fmk was purchased from R&D Systems™. All other chemicals used were purchased from Sigma-Aldrich (Singapore).

General instrumentation. ^{1}H NMR spectrums were obtained using a Bruker Avance 300 spectrometer and the chemical shifts (δ) were reported in parts per million with reference to residual solvent peaks. Electrospray-ionization Mass Spectrometry (ESI-MS) spectra were obtained using Thermo Finnigan MAT ESI-MS System. UV-vis spectra were obtained using the Shimadzu UV-1800 UV Spectrophotometer. Ru concentrations were determined using the Optima ICP-OES (Perkin-Elmer) operated by CMMAC, NUS. Elemental analyses of selected Ru complexes were carried out using a Perkin-Elmer PE 2400 elemental analyzer by CMMAS, NUS. Absorbance on 96-well plates were measured using BioTek® Synergy H1 Hybrid Reader. Western blot proteins bands were visualized *via* enhanced chemiluminescence imaging (PXi, Syngene). Ultrapure water was purified by a Milli-Q UV purification system (Sartorius Stedim Biotech SA).

HPLC analysis of compound purity (assembly yield). Determination of the purity (assembly yield) of 195 RAS complexes was done using analytical HPLC on a Shimadzu Prominence System equipped with a DGU-$20A_3$ Degasser, two LC-20AD Liquid Chromatography Pump, a SPD-20A UV/Vis Detector and a Shim Pack GVP-ODS 2.0 mm 18 column (5 µM, 120Å, 250 mm

x 4.60 mm i.d.) with detection at both 214 nm and 254 nm. The gradient elution conditions were as follows: 20-80% solvent B over 30 min, where solvent A is 10 mM aqueous NH_4OAc pH 7.0 and solvent B is CH_3CN.

C3A Plate Synthesis of RAS complexes. Separate stock solutions containing RA*x* (10 mM), PA*y* (40 mM) and AD*z* (40 mM) were prepared in DMSO. The reactions were then carried out on a Microlon® 200 96-well flat-bottom plate (Greiner Bio-One) with RA*x* (50 µL), PA*y* (25 µL) and AD*z* (25 µL) and ddH_2O (100 µL) added to each well in one portion, yielding RAS complexes (5 mM) in 1:1 v/v DMSO/H_2O (200 µL). The plates were sealed and incubated with shaking at rt for 36 h. This procedure was repeated until all combinations of the three components were achieved. Subsequently, The 195 reaction mixtures were analysed by ESI-MS and RP-HPLC without further work-up or purification.

Cell lines and tissue culture. The human colorectal carcinoma HCT116 and HCT116 $p53^{-/-}$ cell line pair were gifts from Professor Shen Han-ming (NUS). TC7 cells were cloned from parental colorectal adenocarcinoma Caco-2 cells by the limited dilution technique.[2] Human gastric adenocarcinoma AGS cells, were acquired from ATCC® (Manassa,VA). HCT116 and HCT116 $p53^{-/-}$ cells were cultured in DMEM medium containing 10% FBS and 1% Penicillin/Streptomycin. TC7 cells were cultured in DMEM medium containing 20% FBS, 1% Penicillin/Streptomycin and 1% NEAA. AGS cells were cultured in RPMI 1640 medium containing 10% FBS and 1% Penicillin/Streptomycin. All cell lines were grown at 37 °C in a humidified atmosphere of 95% air and 5% CO_2. Experiments were performed on cells within 20 passages.

Inhibition of Cell Viability (Screening). The anti-proliferation activity of the 195 RAS complexes on exponentially growing cancer cells were screened using a modified MTT assay. HCT116 cells and TC7 were seeded at 5000 cells/100 µL per well and 4000 cells/100 µL per well respectively, in Corning® Costar® 96-well plates and incubated for 24 h. Subsequently, the seeded cells were exposed to the library of RAS complexes in a predetermined order, at a single concentration of 25 µM 1% (v/v) DMSO and incubated for 48 h at 37 °C, 5% CO_2. After 48 h, the medium was aspirated and replaced with MTT solution in complete DMEM media (100 µL, 0.5 mg/mL) and incubated for an additional 45 min at 37 °C, 5% CO_2. Subsequently, the medium was aspirated, and the purple formazan crystals dissolved in DMSO (100 µL). The absorbance due to the dissolved purple formazan was than obtained at 570 nm. The cell viabilities associated with each RAS complex were calculated from the measured absorbance of three replicate, with reference to untreated controls.

Synthesis of 532m and 532p. The bulk synthesis of **532m** and **532p** was done in one-pot manner similar to the plate synthesis, except that final volume of the reaction mixture was scaled

up from 200 µL to 20 mL. The DMSO/H_2O solvent mixture was then lyophilized over 48 h. The resulting brown viscous liquid was reconstituted in minimal amount of chloroform and purified by silica gel colomn chromatography (Gradient elution: 1:4 v/v EtOH/$CHCl_3$, R_f = 0.5; 1:3 v/v EtOH/$CHCl_3$, R_f = 0.7). The final product was then dried *in vacuo* for 1 h to give a deep red solid. The products were determined to be > 95% pure by elemental analysis.

532m. Yield: 41 mg (64%). ^{1}H NMR (300 MHz, DMSO-d6): δ 9.34 (s, 1H, py), 8.85 (s, 1H,-C*H*=N-), 8.17 (m, 2H, py+aryl), 8.05 (m, 2H, py+aryl), 7.90 (m, 2H, py+aryl), 5.92 (s, 3H, C_6H_3), 2.61 (s, 3H, py-CH_3), 2.40 (sept, *J* = 7.0 Hz, 3H, C*H*Me_2), 1.14 (d, *J* = 7.0 Hz, 9H, C(CH_3)$_2$), 0.98 (d, *J* = 7.0 Hz, 9H, C(CH_3)$_2$) ppm. ^{13}C NMR (500 MHz, DMSO-d6): δ 171.0, 155.4, 151.6, 151.3, 140.8, 140.1, 130.8, 129.9, 129.6, 126.7, 125.6, 124.7, 122.5, 119.0, 109.1, 80.7, 30.1, 23.4, 20.3, 18.4 ppm. ^{19}F NMR (400 MHz, DMSO-d6): δ -61.3 ppm. ESI-MS (+ve mode): m/z = 605 $[M]^+$. Analysis (Calcd., found for $C_{29}H_{35}Cl_2F_3N_2ORu•4H_2O•0.2CHCl_3$): C (47.62, 47.47), H (5.91, 5.71) N (3.80, 3.52).

532p. Yield: 35.9 mg (56%). ^{1}H NMR (300 MHz, DMSO-d6): δ 9.38 (s, 1H, py), 8.91 (s, 1H, -C*H*=N-), 8.23 (d, *J* = 8.0 Hz, 1H, py), 8.16 (d, *J* = 8.0 Hz, 1H, py), 8.01 (d, *J* = 8.0 Hz, 2H, aryl), 7.90 (d, *J* = 8.0 Hz, 2H, aryl), 5.96 (s, 3H, C_6H_3), 2.62 (s, 3H, py-CH_3), 2.40 (sept, *J* = 7.0 Hz, 3H, C*H*Me_2), 1.13 (d, *J* = 7.0 Hz, 9H, C(CH_3)$_2$), 0.98 (d, *J* = 7.0 Hz, 9H, C(CH_3)$_2$) ppm. ^{13}C NMR (500 MHz, DMSO-d6): δ 170.6, 155.4, 153.9, 151.6, 140.9, 140.1, 130.0, 129.2, 129.0, 126.6, 125.0, 123.3, 122.8, 108.9, 81.0, 30.2, 23.6, 20.3, 18.4 ppm. ^{19}F NMR (400 MHz, DMSO-d6): δ -60.9 ppm. ESI-MS (+ve mode): m/z = 605 $[M]^+$. Analysis (Calcd., found for $C_{29}H_{35}Cl_2F_3N_2ORu•5.5H_2O$): C (47.09, 47.16), H (6.27, 6.10) N (3.79, 3.73).

Inhibition of cell viability assay. The anti-proliferation activities of **532m** and **532p** on exponentially growing cancer cells were determined using MTT assay. HCT116, HCT116 p53$^{-/-}$ and AGS were seeded at 5 000 cells per well (100 µL) while TC7 cells were seeded at 4000 cells per well in Corning® Costar® 96-well plates and incubated for 24 h. Thereafter, cancer cells were exposed to drugs at different concentration in complete media for 48 h. The final concentration of DMSO in medium was < 1% (v/v) at which cell viability was not significantly inhibited. The medium was removed and replaced with MTT solution (100 µL, 0.5 mg/mL) in media and incubated for an additional 45 min. Subsequently, the MTT-medium solution was aspirated, and the purple formazan crystals dissolved in DMSO (100 µL). The absorbance due to the dissolved purple formazan was than obtained at 570 nm. Inhibition to cell viability was evaluated with reference to the IC_{50} value, which is defined as the concentration needed for a 50% reduction of survival based on the survival curves. IC_{50} values were calculated from the dose - response curves obtained in repeated experiments and adjusted to actual [Ru] administered, which was determined using ICP-OES. The experiments were performed in 3 replicates for each drug concentration and were

carried out at least three times independently. For cell viability assays involving inhibitors, z-VAD-fmk (40 µM) was added 1 h prior to the addition of the test compounds and subsequently co-incubated for an additional 48 h. Cell viability in the absence and presence of inhibitor was normalized against the untreated control.

Antibodies and Western blot protocol. HCT116 cells were grown at 500 000 cells per well (2 mL) on Corning® Costar® 6-well plates for 24 h before being treated with **532m** and **532p** at 0.5x and 1x [IC_{50}] for 24 h and 48 h. Oxaliplatin and 5-fluorouracil was used as a positive control at the same effective concentrations. The cells were lysed with RIPA lysis buffer [100 µL, 0.1% SDS, 0.5% Sodium Deoxycholate, 1% IGEPAL® CA-630, 150 mM NaCl, 25 mM Tris-HCl (pH 8.0), protease and phosphatase inhibitor cocktail]. The cell lysates were transferred to separate 1.5 mL tubes and sonicated for 3 x 15 s. The samples were then centrifuged at 13000 rpm, 4˚C for 15 min. The liquid supernatant containing the proteins were collected and total protein content of each sample was quantified *via* Bradford's assay. 50 µg of proteins from each sample were reconstituted in loading buffer [100 mM DTT, 1x Protein Loading Dye] and heated at 95˚C for 5 min. The protein mixtures were resolved on either a 10% or 12% SDS-PAGE gel by electrophoresis and transferred to a 0.2 µm nitrocellulose membrane. Protein bands were visualized *via* enhanced chemiluminescence imaging (PXi, Syngene) after treatment with the appropriate primary and HRP-conjugated secondary antibodies. Equal loading of protein was confirmed by comparison with actin expression. The following antibodies were used: p53 (FL-393) (sc-6243) and p21 (F-5) (sc-6246) from Santa Cruz Biotechnologies. Cleaved caspase-3 (Asp175) (5A1E), cleaved caspase-7 (Asp198) (D6H1), cleaved caspase-9 (Asp330) (D2D4), Parp-1 (46D11), Cleaved Parp-1 (Asp214) (D64E10) and *p*H2A.X (Ser139) (20E3) from Cell Signaling Technology. β-Actin (ab8229) from Abcam. Pierce™ HRP-conguated anti-rabbit IgG (H+L) (#31460), anti-mouse IgG (H+L) (#31430) and anti-goat IgG (H+L) (#31402) from Thermo Fisher Scientific. All antibodies were used at 1:1000 dilutions except for actin (1:10000), anti-mouse, anti-goat and anti-rabbit (1:5000).

SUPPLEMENTARY FIGURES

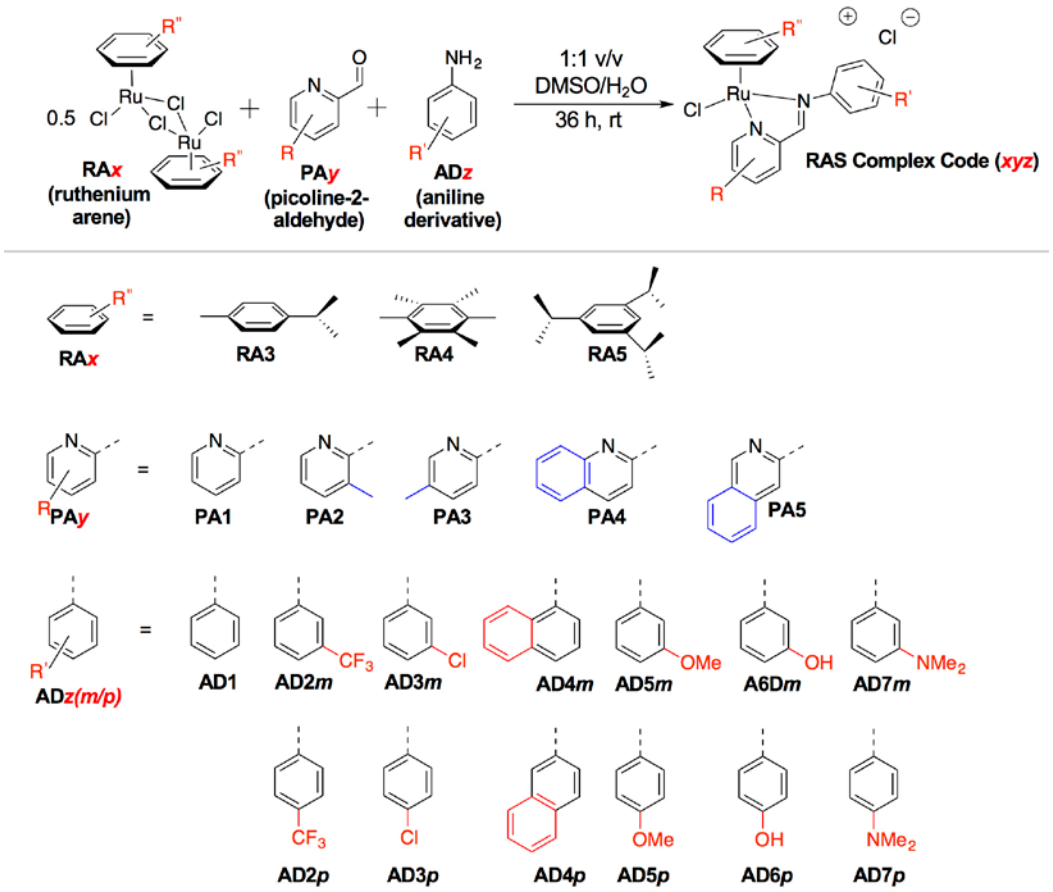

Figure S1. Structures and naming convention for 195 RAS complexes. RAS complexes in the subsequent figures are named according to this standardized convention.

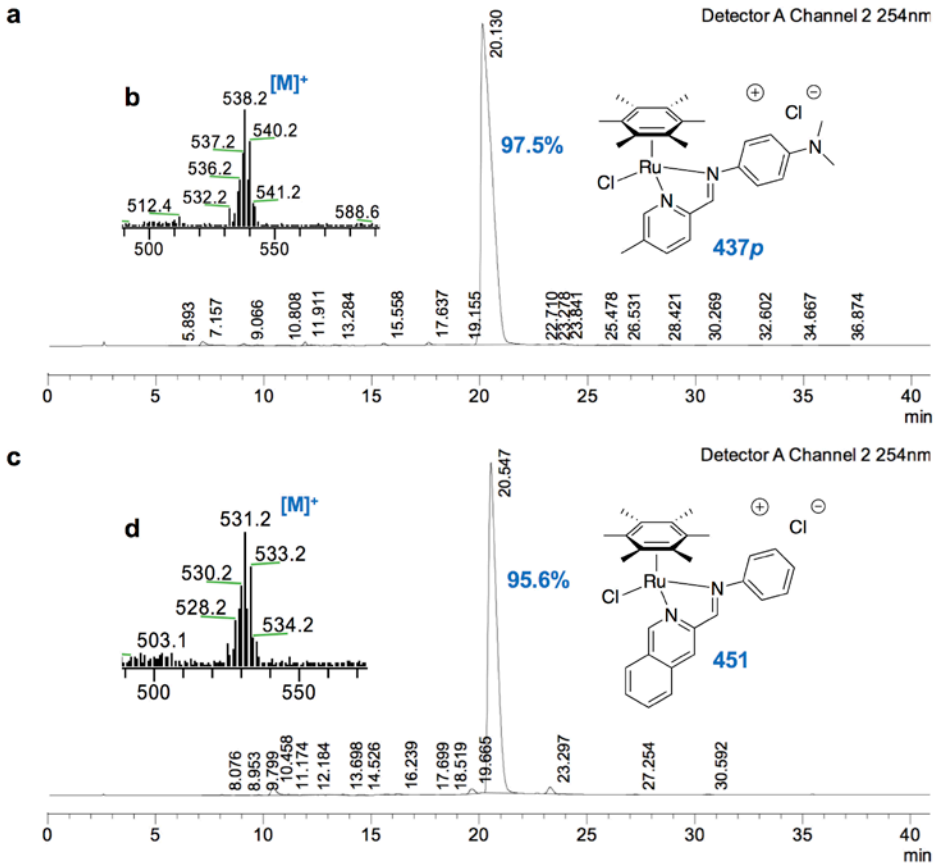

Figure S2. Examples of ESI-MS and HPLC spectrums for assembled RAS complexes. (**a**) HPLC spectrum and (**b**) ESI-MS spectrum of **437p**. (**c**) HPLC Spectrum and (**d**) ESI-MS spectrum of **451**. Samples were analyzed immediately after C3A one-pot synthesis without further work-up or purification.

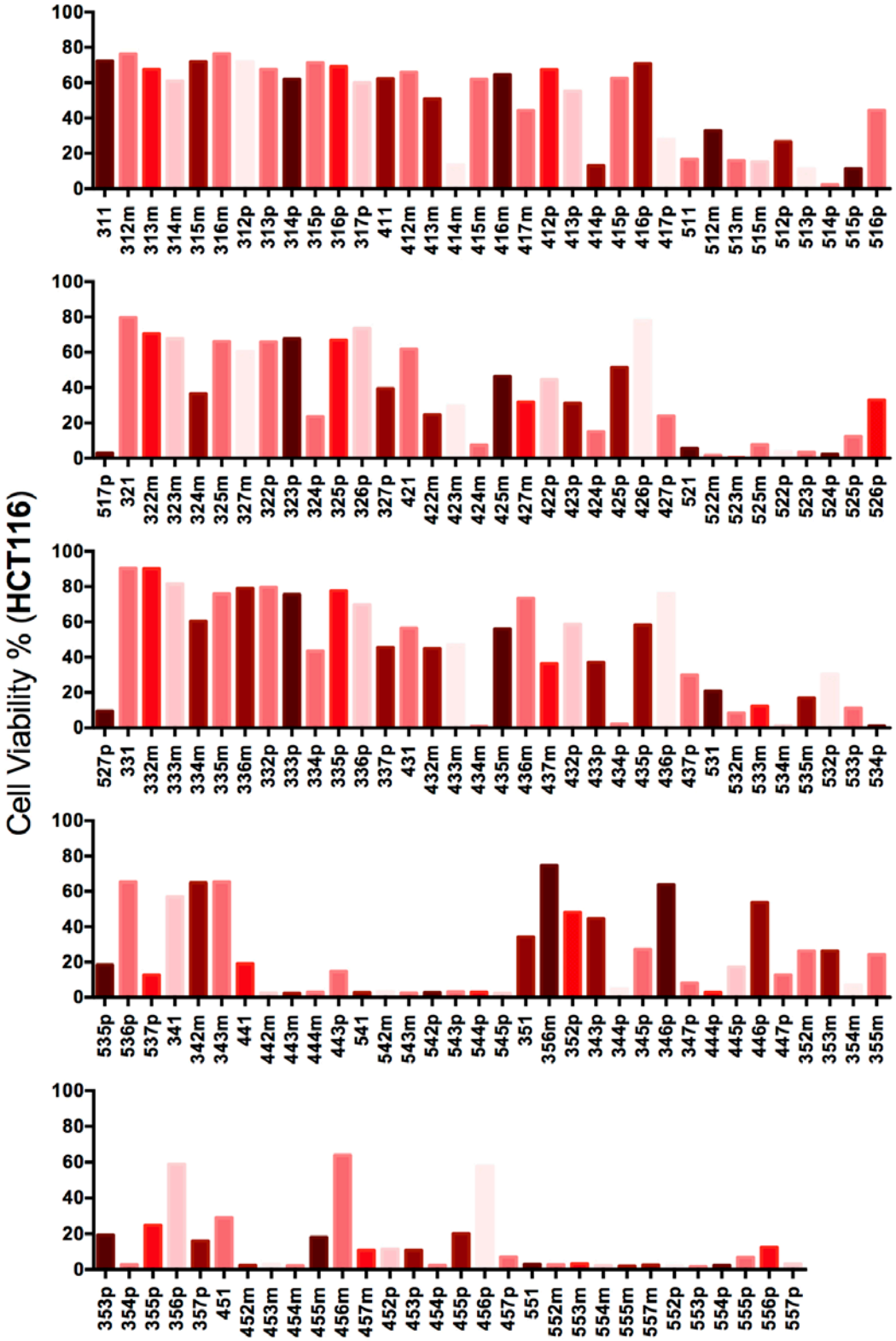

Figure S3. HCT116 cell viability %, 48h after single-concentration screen (25 μM) with 166 RAS complexes. Only compounds with assembly yield (purity) greater than 70% were chosen for the screen.

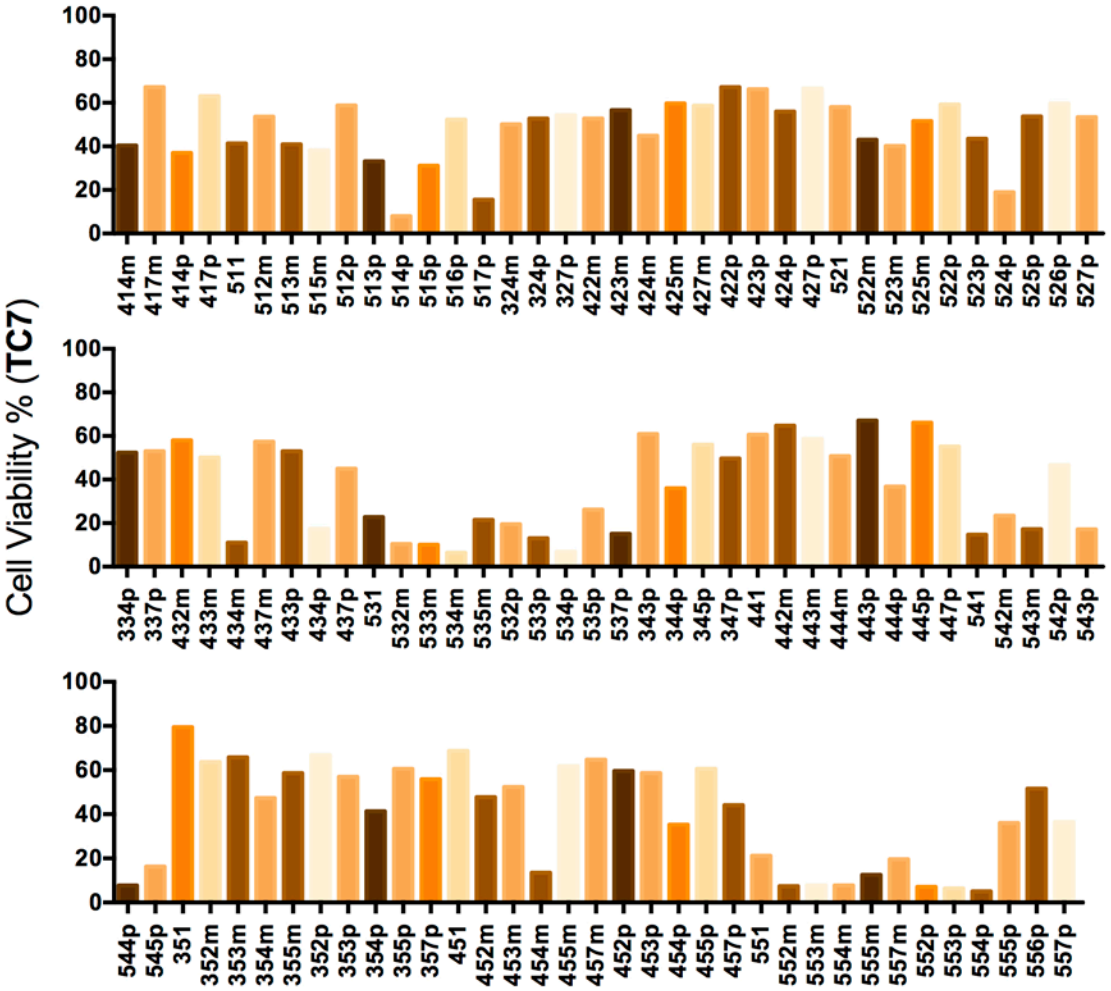

Figure S4. TC7 cell viability %, 48h after single-concentration screen (25 μM) with 107 RAS complexes. Only compounds with assembly yield (purity) greater than 70% and cell viability lesser than 50% in HCT116 were chosen for the screen.

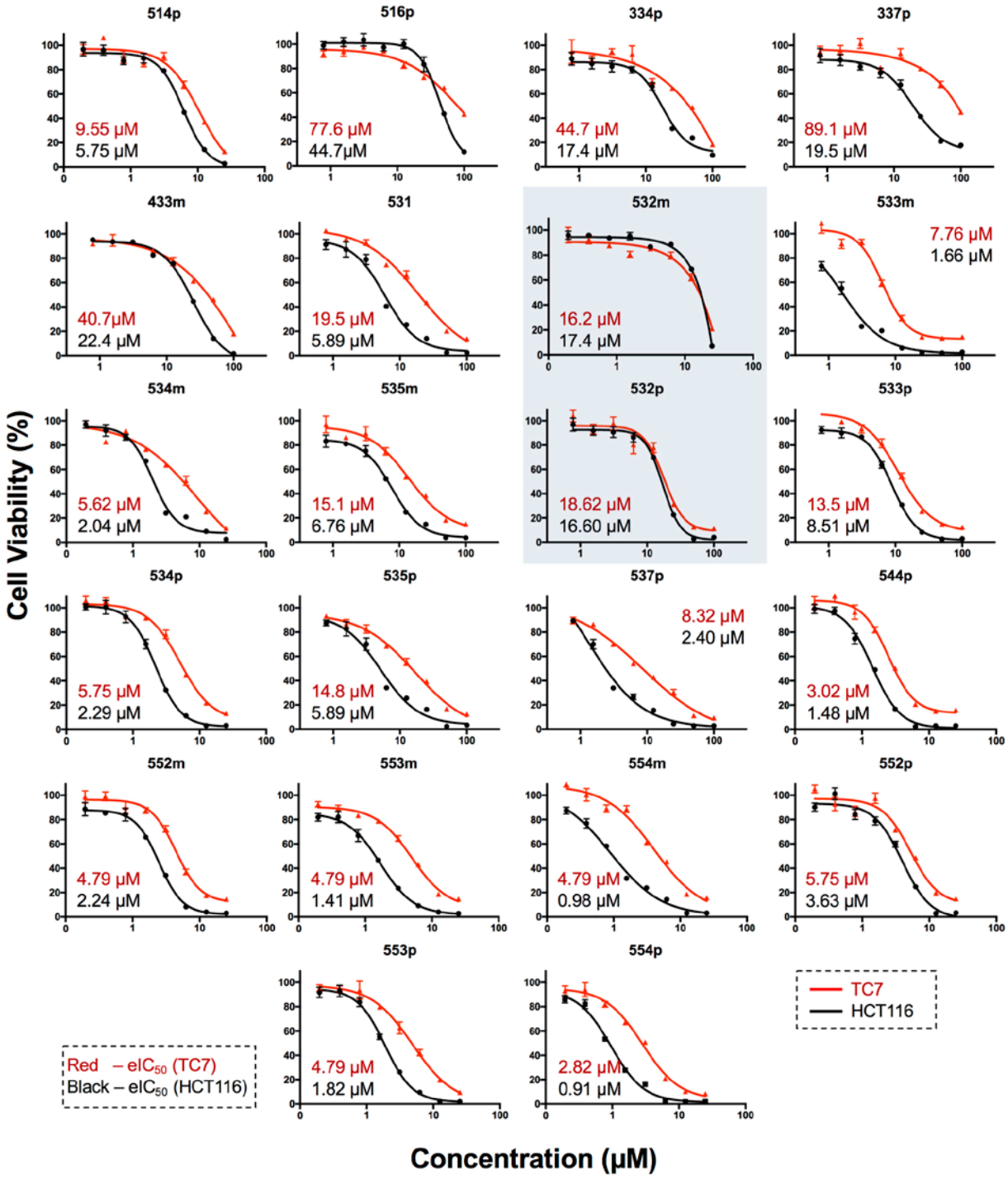

Figure S5. Cell viability curves from secondary screening. 22 initial hits from the single-concentration screens were tested at a range of concentrations in both HCT116 (apoptosis-sensitive) and TC7 (apoptosis-resistant) to obtain their cell viability curves. The estimated IC_{50} values from one set of experiments was used to identify the two apoptosis-independent lead compound, **532m** and **532p**.

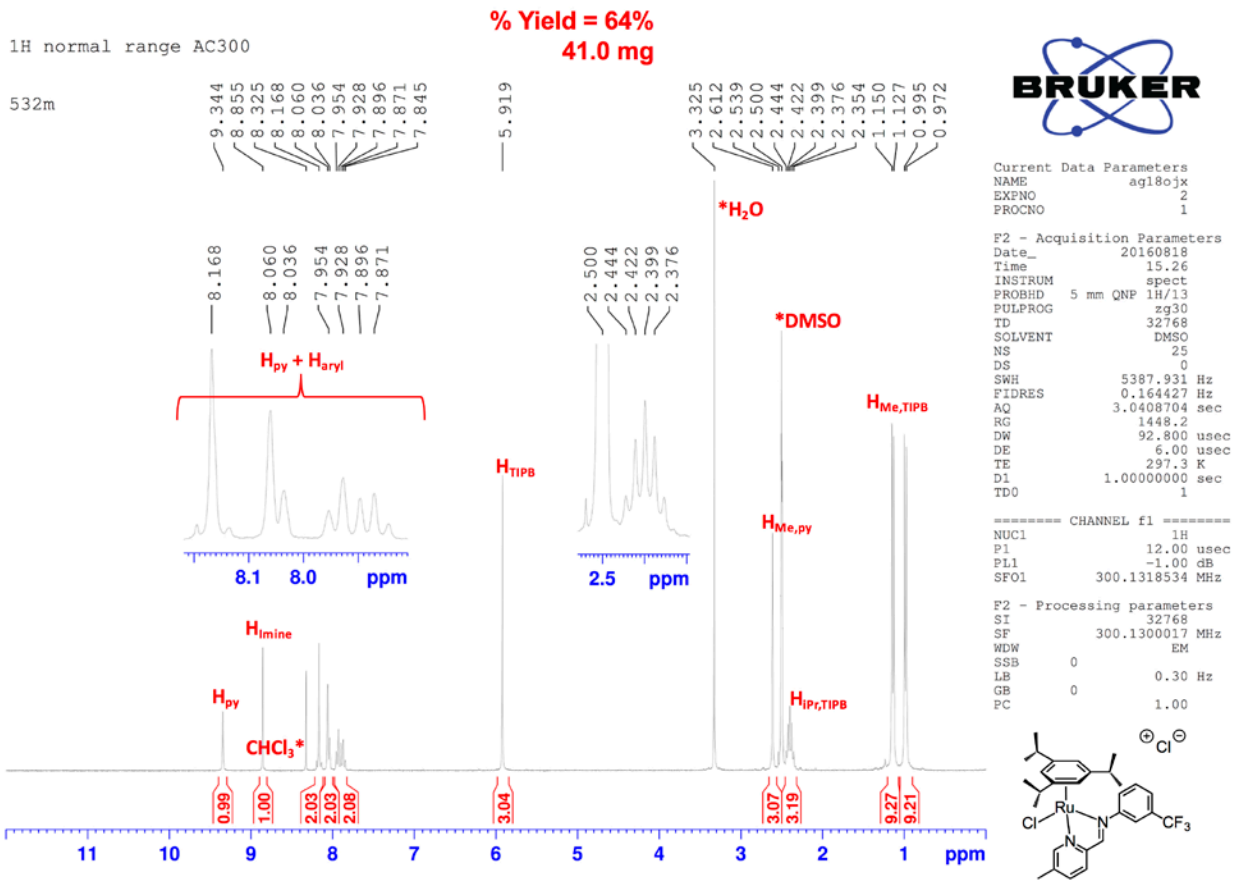

Figure S6. ^{1}H NMR spectrum of 532m. Spectrum was acquired using a 300 MHz spectrometer in DMSO-d6. The formation of the imine peak around 9.0 ppm is indicative of the formation of the complex. Residual solvent peaks are as indicated.

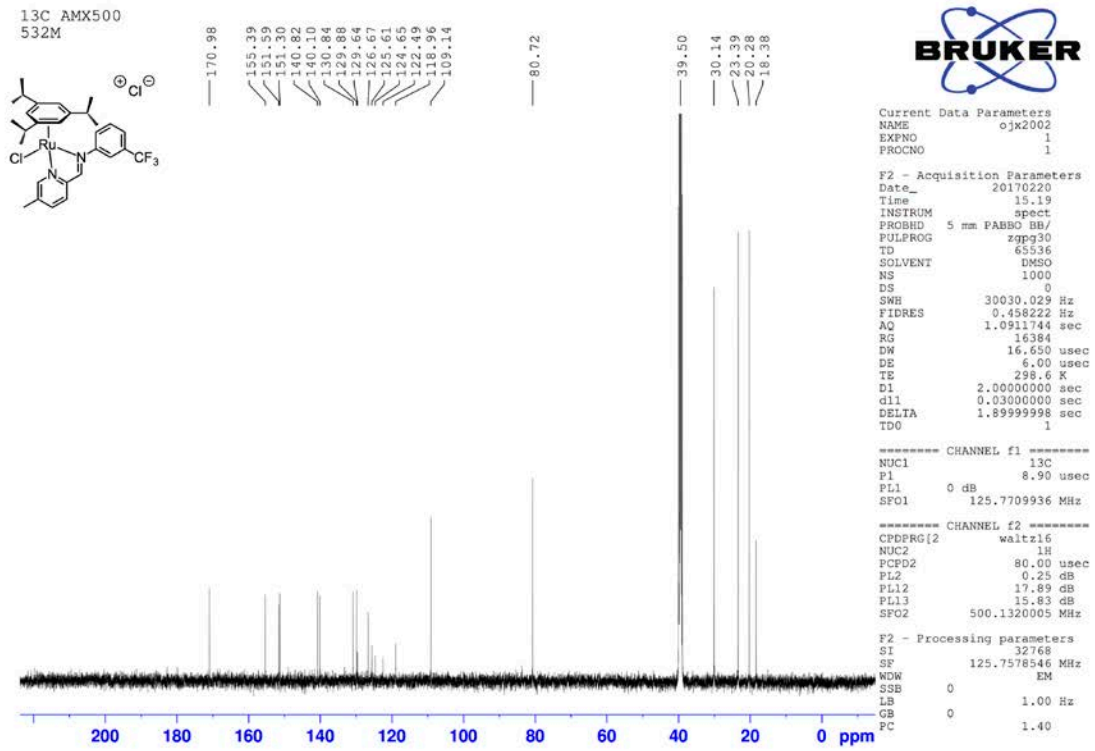

Figure S7. ^{13}C NMR spectrum of 532m. Spectrum was acquired using a 500 MHz spectrometer in DMSO-d6.

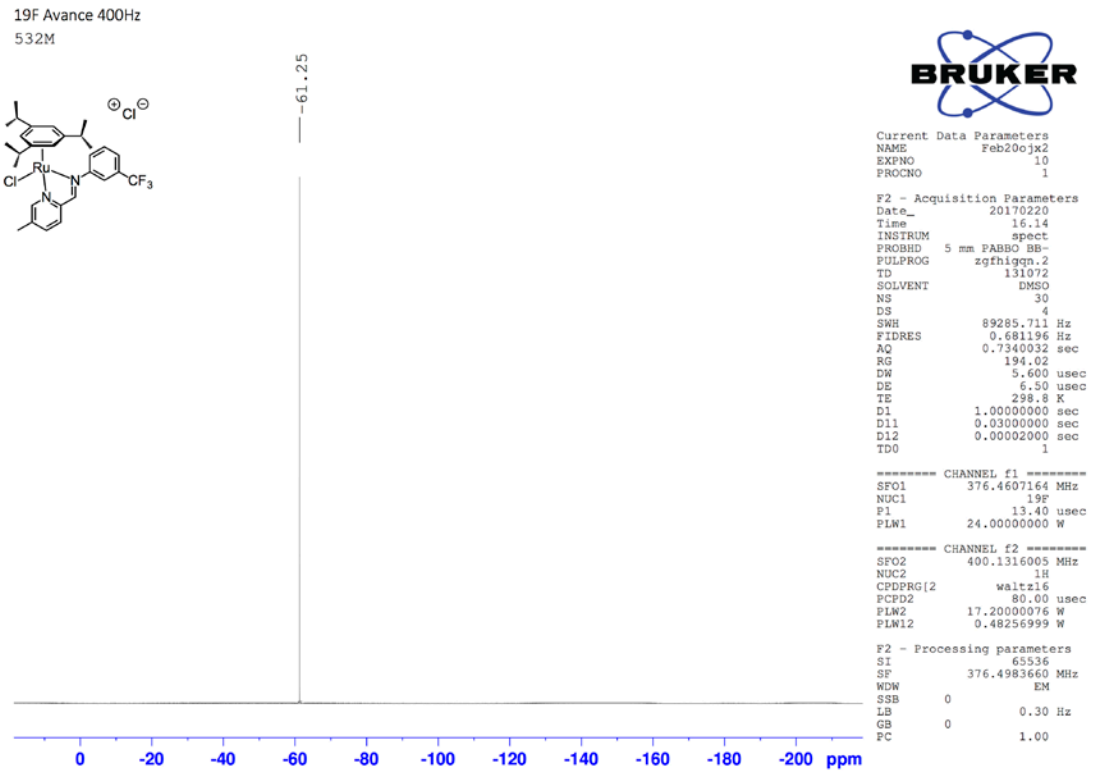

Figure S8. ^{19}F NMR spectrum of 532m. Spectrum was acquired using a 400 MHz spectrometer in DMSO-d6.

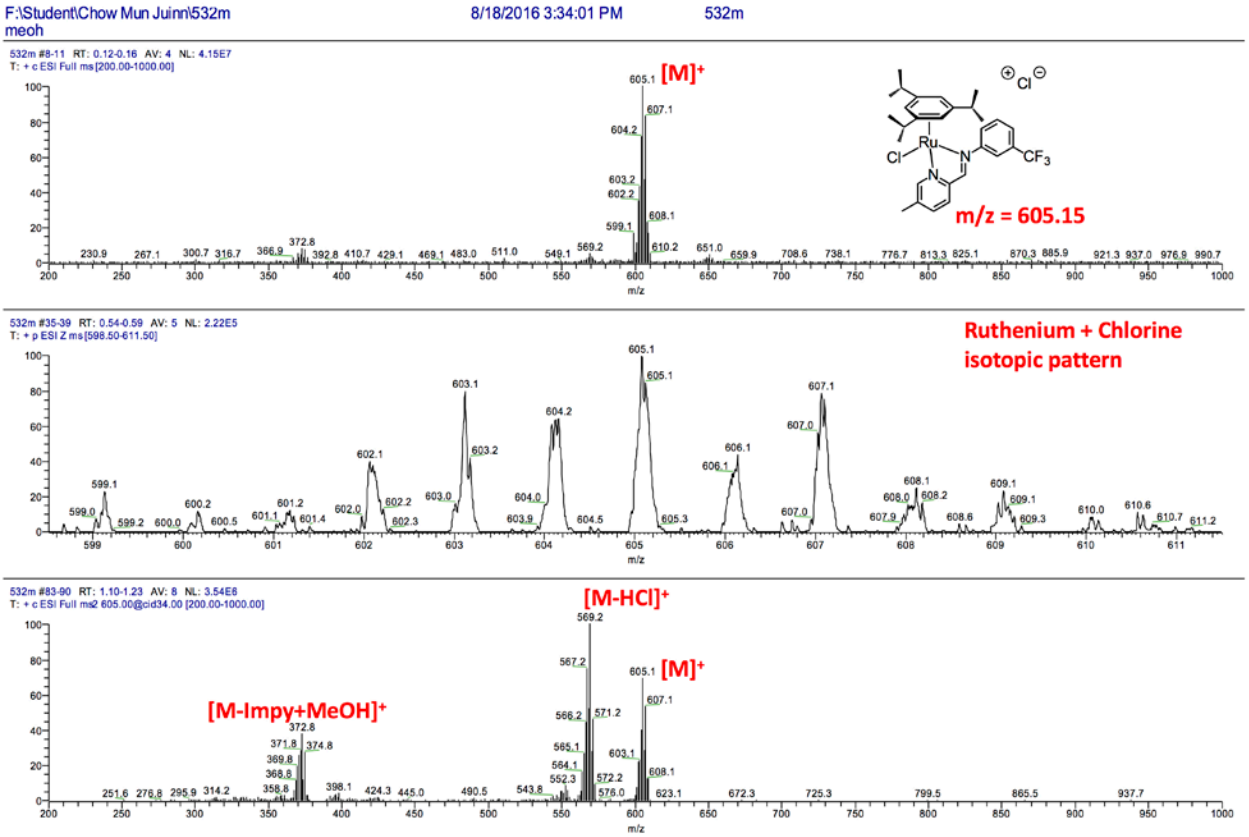

Figure S9. ESI-MS spectrum of 532m. (Top panel) Full MS spectrum; (Middle panel) Zoom Scan of molecular ion peak. Ruthenium and chloride isotope pattern is observed; (Bottom panel) Tandem MS-MS spectrum. Expected fragmentation pattern was observed.

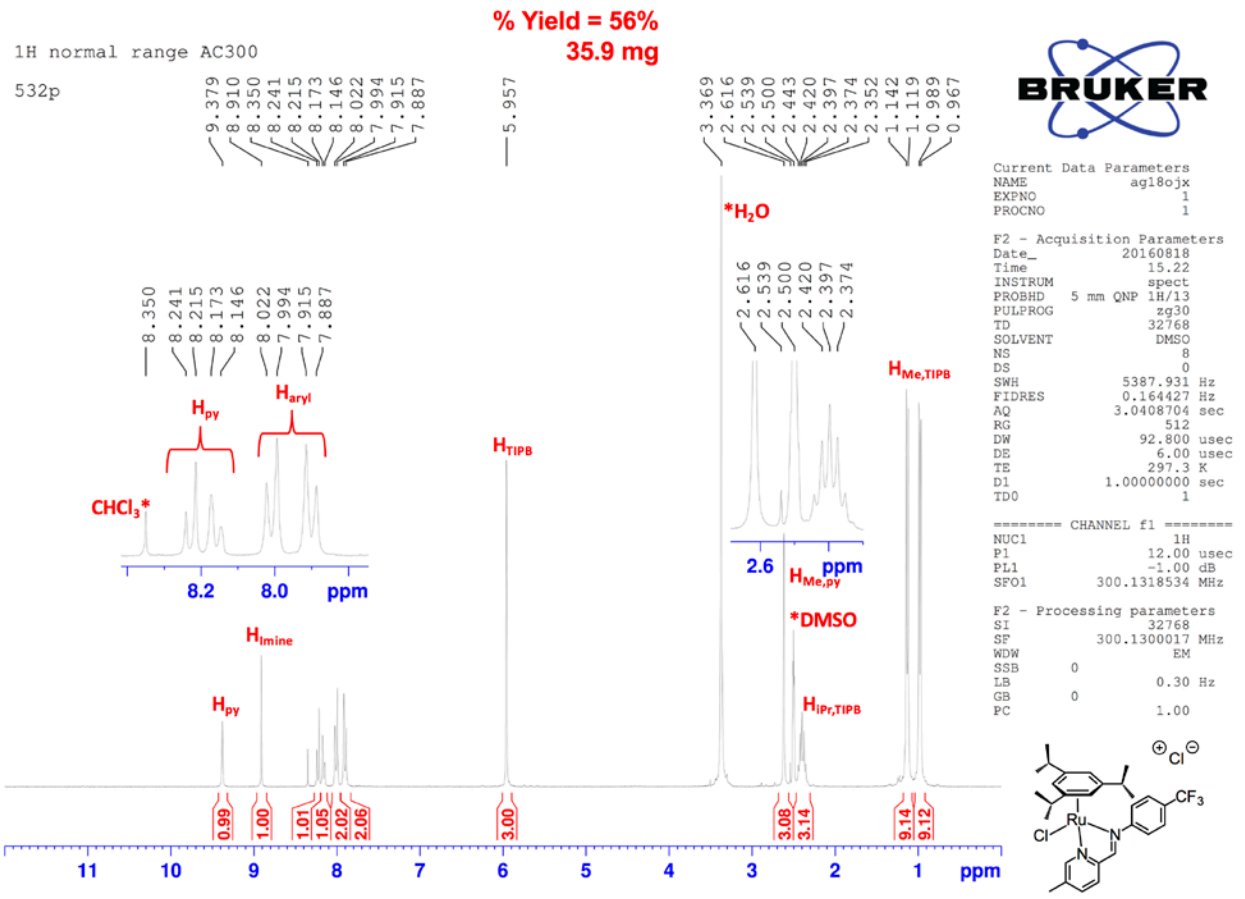

Figure S10. ^{1}H NMR spectrum of 532p. Spectrum was acquired using a 300 MHz spectrometer in DMSO-d6. The formation of the imine peak around 9.0 ppm is indicative of the formation of the complex. Residual solvent peaks are as indicated.

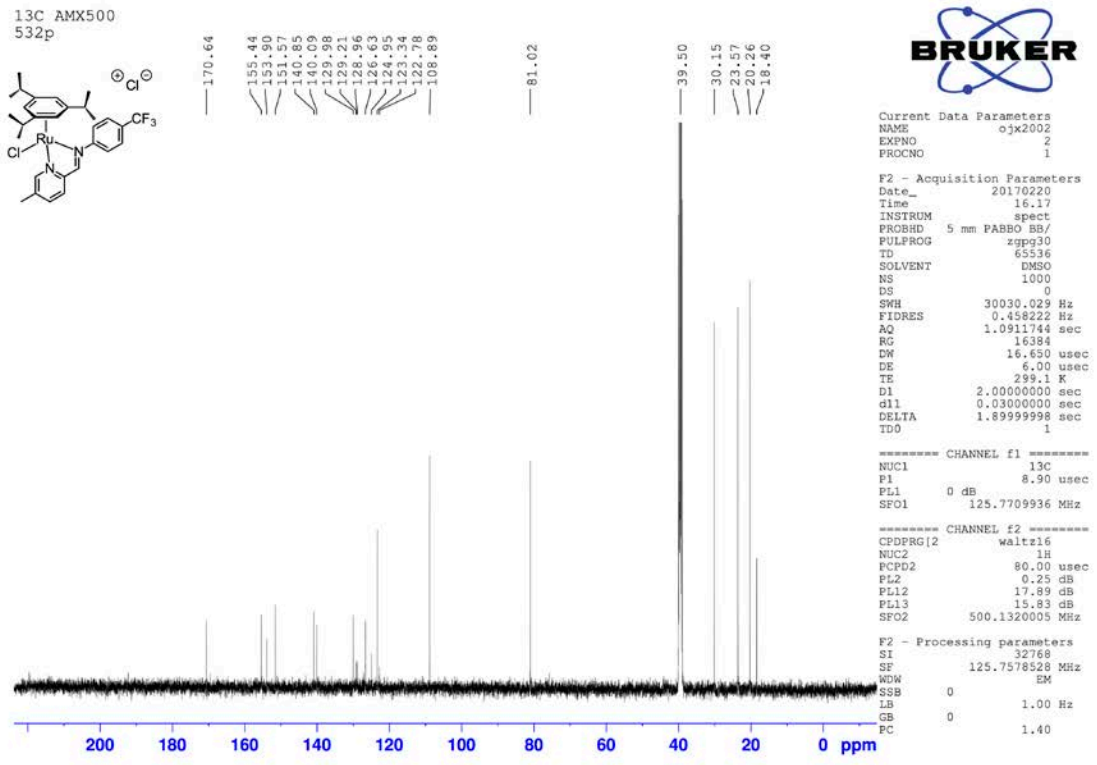

Figure S11. ^{13}C NMR spectrum of 532p. Spectrum was acquired using a 500 MHz spectrometer in DMSO-d6.

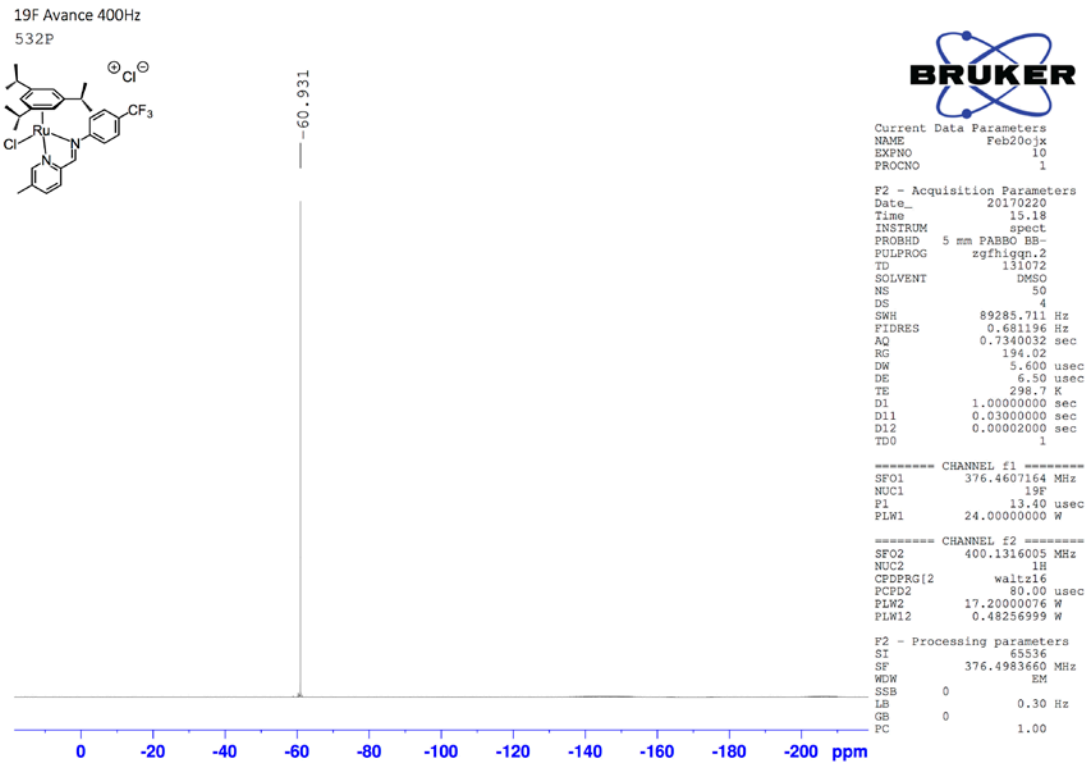

Figure S12. ^{19}F NMR spectrum of 532p. Spectrum was acquired using a 500 MHz spectrometer in DMSO-d6.

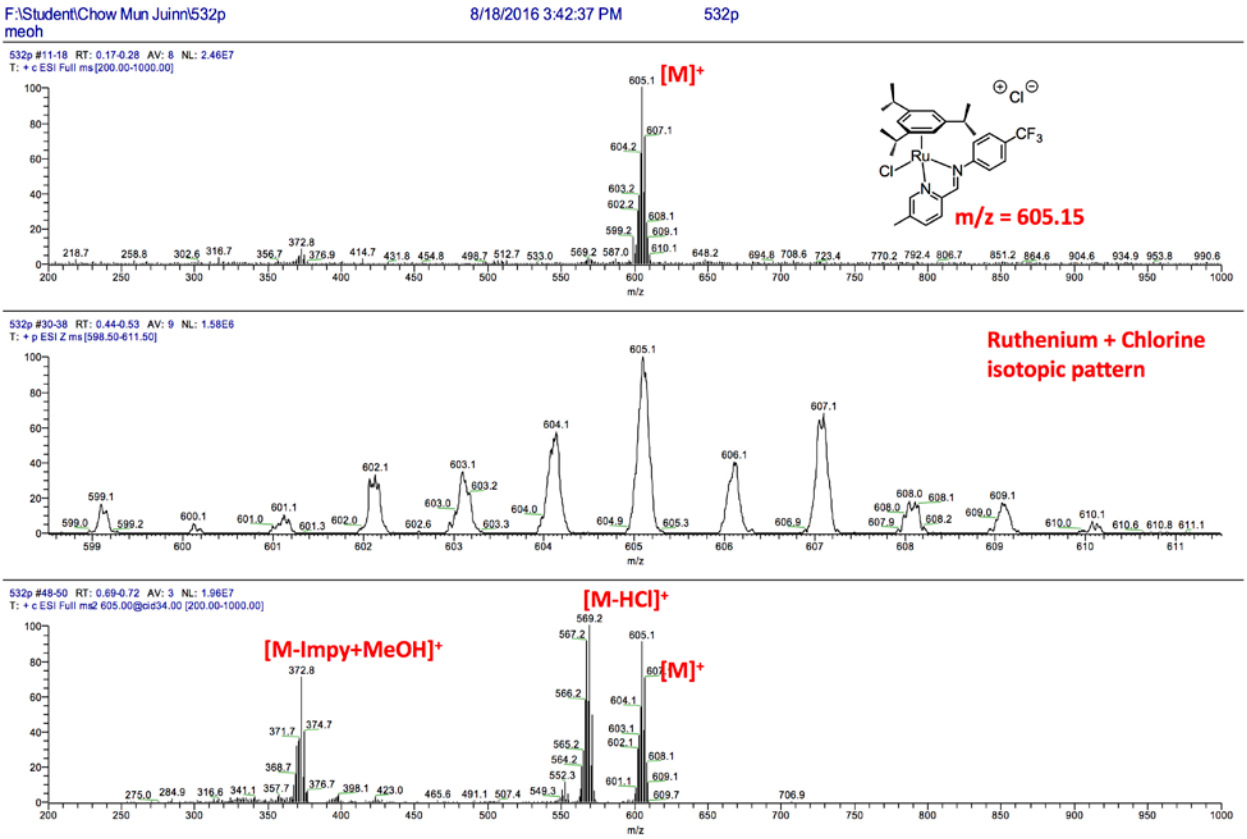

Figure S13. ESI-MS spectrum of 532p. (Top panel) Full MS spectrum; (Middle panel) Zoom Scan of molecular ion peak. Ruthenium and chloride isotope pattern is observed; (Bottom panel) Tandem MS-MS spectrum. Expected fragmentation pattern was observed.

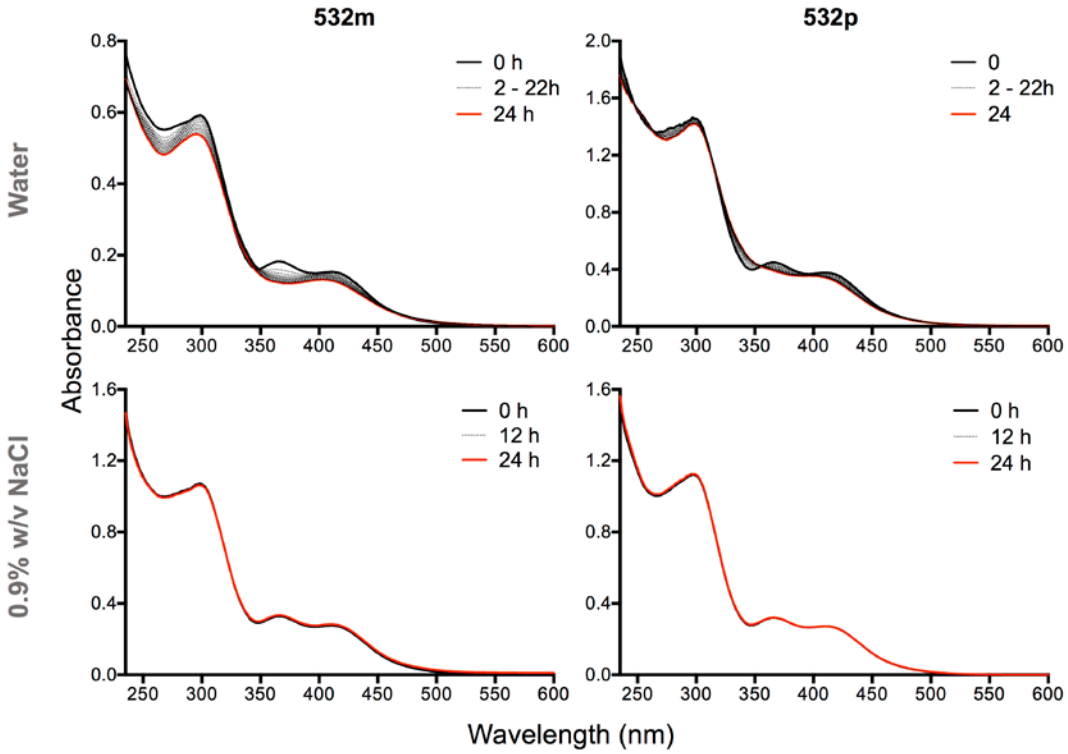

Figure S14. Stability studies of 532m and 532p. The UV-vis profile of the two lead compounds were monitored over 24 h in water and 0.9% w/v NaCl. (Top panels) Shifts in UV-vis profile of both compounds, with the formation of multiple isosbestic points, were observed in water; (Bottom panels) No shift was observed in 0.9% w/v NaCl. The spectrums show that **532m** and **532p** undergo some degree of aquation in water, which could be suppressed by chloride concentration similar to that of physiological conditions.

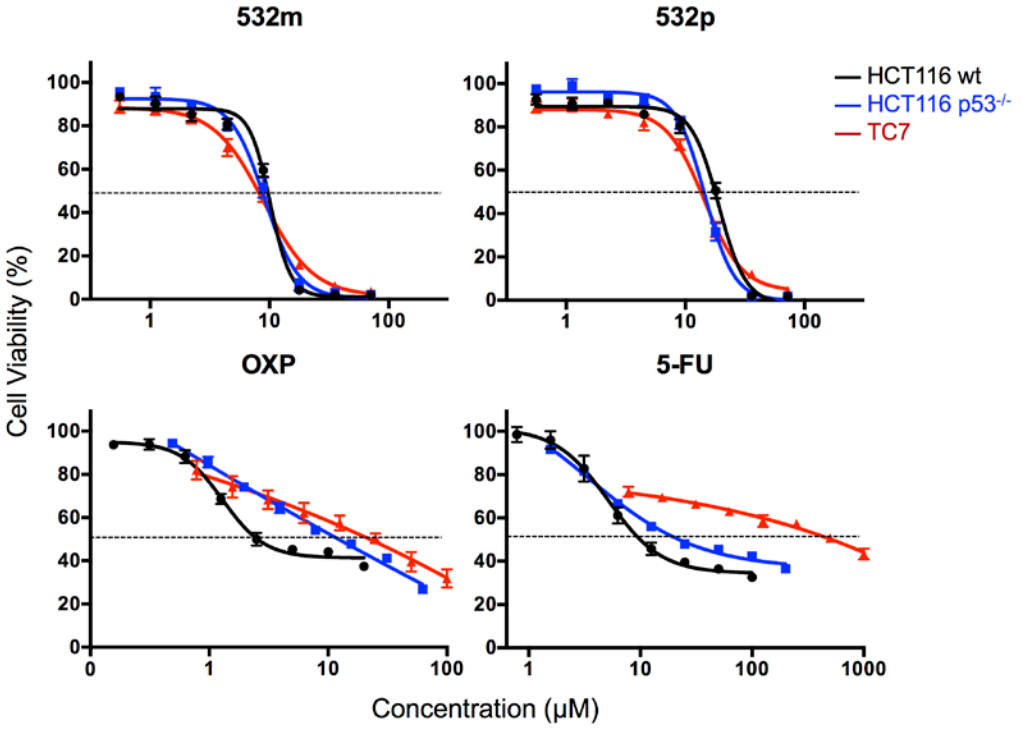

Figure S15. Comparison of cell viability curves from three different cell line. Each curve shown is the average of three independent experiment. **532m** and **532p** showed similar toxicity profile in all three cell lines. In contrast, oxaliplatin and 5-fluorouracil showed decreased efficacy in p53-null (HCT116 $p53^{-/-}$) and apoptosis-resistant (TC7) cell lines.

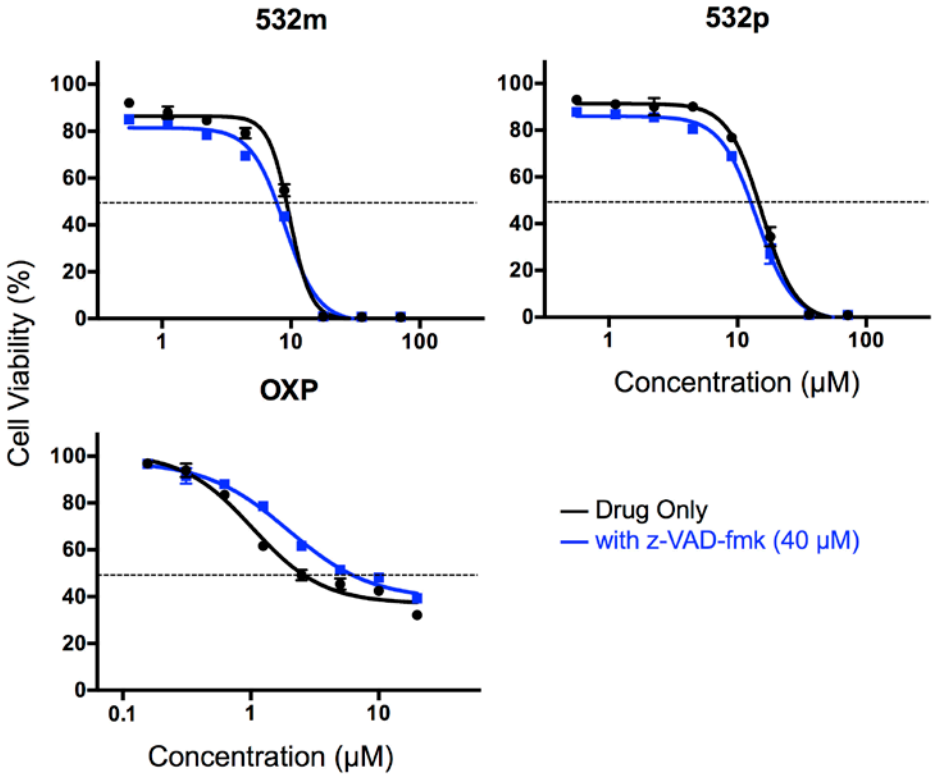

Figure S16. Comparison of HCT116 cell viability curves with and without pan-caspase inhibitor z-VAD-fmk. Each curve shown is the average of three independent experiment. **532m** and **532p** showed similar toxicity profile with and without z-VAD-fmk. In contrast, oxaliplatin showed decreased efficacy when co-incubated with z-VAD-fmk (with 1h pre-incubation).

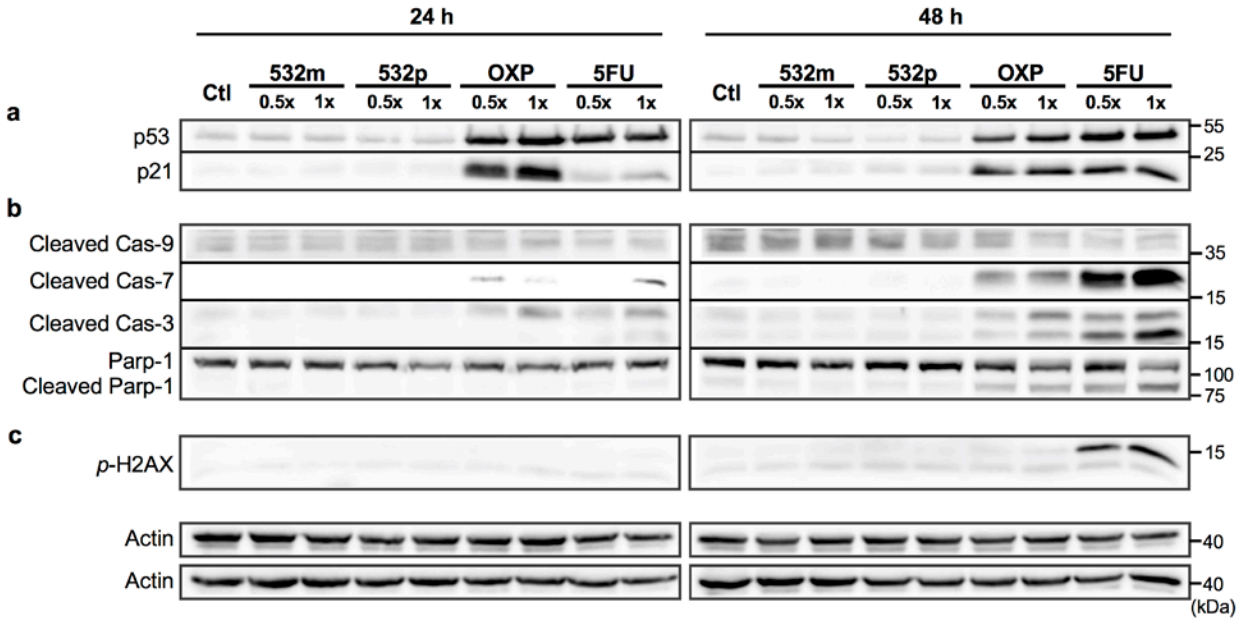

Figure S17. Western blot analysis after treatment with 532m, 532p and positive controls. (**a**) p53 and p53-target protein. (**b**) Apoptosis biomarkers. (**c**) Biomarker for DNA damage. Homogeneous protein loading determined with reference to actin.

SUPPLEMENTARY TABLE

Table S1. % Assembly Yield (Purity) of each RAS complex, determined by HPLC analysis.

% Yield

PA1	RA3	RA4	RA5		RA3	RA4	RA5
AD1	95	93	93				
AD2m	90	92	81	AD2p	92	90	78
AD3m	92	92	87	AD3p	95	95	89
AD4m	82	87	65	AD4p	94	94	89
AD5m	93	89	87	AD5p	94	93	91
AD6m	77	82	47	AD6p	98	93	92
AD7m	64	74	63	AD7p	93	95	88

PA2	RA3	RA4	RA5		RA3	RA4	RA5
AD1	93	92	87				
AD2m	90	94	80	AD2p	88	87	74
AD3m	93	90	86	AD3p	94	95	84
AD4m	83	89	63	AD4p	93	95	84
AD5m	89	87	79	AD5p	91	89	83
AD6m	46	60	-	AD6p	92	91	85
AD7m	72	76	62	AD7p	93	94	84

PA3	RA3	RA4	RA5		RA3	RA4	RA5
AD1	93	94	91				
AD2m	93	96	87	AD2p	85	94	84
AD3m	96	93	88	AD3p	93	97	81
AD4m	81	91	71	AD4p	94	95	85
AD5m	91	90	87	AD5p	94	97	89
AD6m	82	84	58	AD6p	93	95	89
AD7m	66	74	54	AD7p	96	98	82

PA4	RA3	RA4	RA5		RA3	RA4	RA5
AD1	83	81	80				
AD2m	75	82	77	AD2p	66	56	70
AD3m	77	77	80	AD3p	83	79	72
AD4m	55	70	57	AD4p	79	76	75
AD5m	68	56	61	AD5p	78	84	75
AD6m	45	44	32	AD6p	79	80	68
AD7m	-	-	-	AD7p	71	74	61

PA5	RA3	RA4	RA5		RA3	RA4	RA5
AD1	94	96	90				
AD2m	91	95	86	AD2p	89	79	89
AD3m	92	94	92	AD3p	88	96	86
AD4m	73	82	75	AD4p	92	94	83
AD5m	91	93	87	AD5p	96	95	88
AD6m	74	87	59	AD6p	90	93	89
AD7m	69	82	75	AD7p	89	93	81

	%	Number	%	%
> 70	>90	76	39	85
	70-89	90	46	
<70	50-69	20	10	15
	<50	9	5	
	Total	195	100	100

Table S2. HCT116 cell viability data after single-concentration (25 µM) screen with 166 RAS complexes of sufficient purity.

% CV	HCT116

PA1	RA3	RA4	RA5		RA3	RA4	RA5
AD1	72	62	17				
AD2m	76	66	33	AD2p	72	68	27
AD3m	68	51	16	AD3p	68	55	11
AD4m	61	13		AD4p	62	13	2
AD5m	72	62	15	AD5p	71	63	11
AD6m	76	64		AD6p	69	71	44
AD7m		44		AD7p	60	28	3

PA2	RA3	RA4	RA5		RA3	RA4	RA5
AD1	80	62	6				
AD2m	71	25	2	AD2p	66	44	4
AD3m	68	29	0	AD3p	68	31	3
AD4m	37	7		AD4p	24	15	2
AD5m	66	46	8	AD5p	67	51	12
AD6m				AD6p	73	78	33
AD7m	60	32		AD7p	39	24	9

PA3	RA3	RA4	RA5		RA3	RA4	RA5
AD1	90	57	21				
AD2m	90	45	8	AD2p	80	58	30
AD3m	81	47	12	AD3p	75	37	11
AD4m	60	1	1	AD4p	43	2	1
AD5m	76	56	17	AD5p	78	58	18
AD6m	79	73		AD6p	70	76	65
AD7m		36		AD7p	45	30	13

PA4	RA3	RA4	RA5		RA3	RA4	RA5
AD1	57	19	3				
AD2m	65	3	3	AD2p			3
AD3m	65	2	2	AD3p	45	15	3
AD4m		3		AD4p	5	3	3
AD5m				AD5p	27	17	2
AD6m				AD6p	64	54	
AD7m				AD7p	8	13	

PA5	RA3	RA4	RA5		RA3	RA4	RA5
AD1	34	29	3				
AD2m	26	2	3	AD2p	48	11	2
AD3m	26	3	3	AD3p	19	11	2
AD4m	7	2	2	AD4p	3	2	2
AD5m	24	18	2	AD5p	25	20	7
AD6m	75	64		AD6p	59	58	13
AD7m		11	3	AD7p	16	7	3

	%	Number	%	%
> 50	>50	59	36	48
	30-49	21	13	
< 50	10-29	39	23	52
	<10	47	28	
	Total	166	100	100

Table S3. TC7 cell viability data after single-concentration (25 µM) screen with 107 RAS complexes, chosen with reference to the cell viability data from HCT116.

% CV	TC7

PA1	RA3	RA4	RA5		RA3	RA4	RA5
AD1			41				
AD2m			54	AD2p			59
AD3m			41	AD3p			33
AD4m		40		AD4p		37	8
AD5m			38	AD5p			31
AD6m				AD6p			52
AD7m		67		AD7p		63	16

PA2	RA3	RA4	RA5		RA3	RA4	RA5
AD1			58				
AD2m		53	43	AD2p		67	59
AD3m		57	40	AD3p		66	44
AD4m	50	45		AD4p	53	56	19
AD5m		60	52	AD5p			54
AD6m				AD6p			60
AD7m		59		AD7p	54	67	53

PA3	RA3	RA4	RA5		RA3	RA4	RA5
AD1			23				
AD2m		58	10	AD2p			20
AD3m		50	10	AD3p		53	13
AD4m		11	6	AD4p	52	17	7
AD5m			22	AD5p			26
AD6m				AD6p			
AD7m		57		AD7p	53	45	15

PA4	RA3	RA4	RA5		RA3	RA4	RA5
AD1		61	15				
AD2m		65	23	AD2p			47
AD3m		59	17	AD3p	61	67	17
AD4m		51		AD4p	36	37	8
AD5m				AD5p	56	66	16
AD6m				AD6p			
AD7m				AD7p	50	55	

PA5	RA3	RA4	RA5		RA3	RA4	RA5
AD1	79	69	21				
AD2m	64	48	7	AD2p	67	60	7
AD3m	66	52	8	AD3p	57	59	6
AD4m	47	13	8	AD4p	41	35	5
AD5m	59	62	12	AD5p	61	61	36
AD6m				AD6p			52
AD7m		65	20	AD7p	56	44	36

	%	Number	%	%
> 50	>50	54	50	71
	30-49	22	21	
< 50	10-29	20	19	29
	<10	11	10	
	Total	107	100	100

REFERENCES

1. M. J. Chow, C. Licona, D. Y. Q. Wong, G. Pastorin, C. Gaiddon and W. H. Ang, *J. Med. Chem.*, 2014, **57**, 6043-6059.
2. I. Chantret, A. Rodolosse, A. Barbat, E. Dussaulx, E. Brot-Laroche, A. Zweibaum and M. Rousset, *J. Cell Sci.*, 1994, **107**, 213-225.